

See discussions, stats, and author profiles for this publication at: <https://www.researchgate.net/publication/256446211>

Enantiospecific Kinetics in Surface Adsorption: Propylene Oxide on Pt(111) Surfaces

ARTICLE *in* THE JOURNAL OF PHYSICAL CHEMISTRY C · AUGUST 2013

Impact Factor: 4.77 · DOI: 10.1021/jp406495w

CITATIONS

4

READS

67

5 AUTHORS, INCLUDING:



[Stavros Karakalos](#)

Harvard University

33 PUBLICATIONS 72 CITATIONS

[SEE PROFILE](#)



[Timothy Lawton](#)

Tufts University

21 PUBLICATIONS 251 CITATIONS

[SEE PROFILE](#)



[Charles Sykes](#)

Tufts University

114 PUBLICATIONS 1,708 CITATIONS

[SEE PROFILE](#)



[Francisco Zaera](#)

University of California, Riverside

377 PUBLICATIONS 12,326 CITATIONS

[SEE PROFILE](#)

Enantiospecific Kinetics in Surface Adsorption: Propylene Oxide on Pt(111) Surfaces

Stavros Karakalos,[†] Timothy J. Lawton,[‡] Felicia R. Lucci,[‡] E. Charles H. Sykes,[‡] and Francisco Zaera^{†,*}

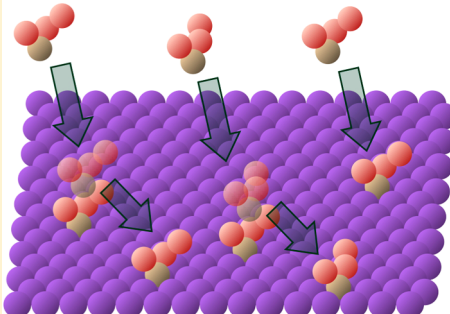
[†]Department of Chemistry, University of California, Riverside, California 92521, United States

[‡]Department of Chemistry, Tufts University, Medford, Massachusetts 02155, United States

Supporting Information

ABSTRACT: The enantiomers of chiral compounds are mirror images of each other and therefore exhibit identical chemical and physical properties. However, many mixtures of enantiomers of single chiral compounds exhibit different properties than those of each of the enantiomers alone. This is because opposite enantiomers usually pair up and form racemic compounds via strong interactions such as hydrogen bonding. Here we report on a unique case where the differences are due to a kinetic effect instead. The saturation monolayer of a racemic (50:50) mixture of propylene oxide on a Pt(111) surface was found to be approximately 20% less dense than a similar layer made out of one single propylene oxide enantiomer. A combination of temperature programmed desorption, scanning tunneling microscopy and molecular beam experiments and kinetic Monte Carlo simulations were used to identify the reason for this behavior to be adsorbate-assisted kinetics adsorption with different probabilities for homo- versus heteroenantiomeric pairs.

$$S_{RR}, S_{SS} > S_{RS}, S_{SR} > S_{\text{empty}}$$



1. INTRODUCTION

When carbon atoms in organic molecules are bonded to four different moieties, the resulting chiral compounds can exist in one of two equivalent but nonsuperimposable enantiomeric forms. These enantiomers are mirror images with opposite handedness, and show identical chemical and physical properties in achiral environments. However, when two enantiomers interact with each other, differences in their relative handedness can lead to differences in chemical or physical behavior. This is why enantioselectivity is so important in biological systems: much of the biochemistry that sustains life involves single enantiomers of chiral molecules, and any chemicals meant to react with those, pharmaceuticals in particular, need to show the appropriate enantioselectivity to elicit the desired beneficial effect.¹

The differences in behavior between combinations of enantiomers of the same versus the opposite handedness extend to mixtures of individual single chiral compounds.² For instance, while the normal melting point of enantiomerically pure D- or L-menthol is 316 K, racemic DL-menthol mixtures melt at 307 K.³ This is because racemic menthol forms a 1:1 racemic compound (racemate) in the solid phase. In fact, approximately 90–95% of the racemic mixtures of chiral organic molecules follow similar crystallization behavior.^{4,5} Most of the remaining systems form solid conglomerates instead, with each enantiomer condensing separately to produce mixtures of enantiomerically pure crystals; the observation of this behavior with tartaric acid is what led Pasteur to the discovery of molecular chirality.⁶ Because most chiral compounds exhibit strong intermolecular interactions

such as hydrogen bonding, the choice between these two options, namely, racemate versus conglomerate formation, is determined by the relative strength of the interactions between enantiomers of the same versus opposite handedness. There is a third option for chiral compounds, the formation of solid solutions, but those are quite rare (~1%), and even there strong intermolecular interactions are typical, only they with similar strengths in homo- versus heteroenantiomeric mixtures.⁷

Herein, we report on a chiral system where enantiopure and racemic mixtures exhibit different physical properties despite the lack of strong intermolecular interactions. Specifically, temperature-programmed desorption (TPD) data showed that the density of the saturated monolayers of propylene oxide (PO) adsorbed on a Pt(111) single-crystal surface changes monotonically with enantiomeric composition, decreasing by approximately 20% when going from enantiopure to racemic layers. Scanning tunneling microscopy (STM) images were used to corroborate the coverage changes, and also to reveal that there is no racemate formation or long-range ordering on these surfaces. It was found that the density of the racemic PO layers could be increased slightly if the uptake is carried out at higher temperatures, an indication that the observed behavior is kinetically controlled. However, this effect was found to be limited by competition with desorption from the surface. Data from isothermal molecular-beam measurements indicated that

Received: July 1, 2013

Revised: August 9, 2013

Published: August 29, 2013

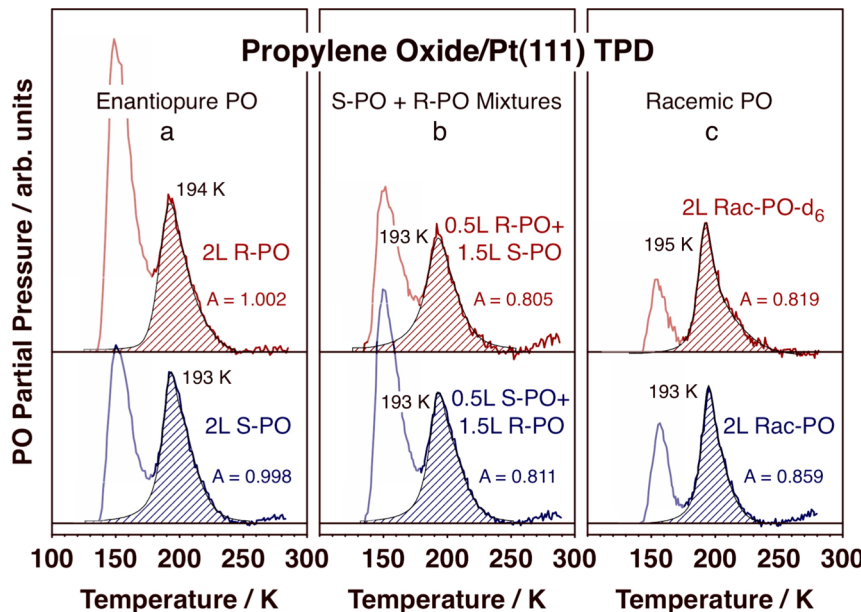


Figure 1. Temperature-programmed desorption (TPD) data for propylene oxide (PO) molecular desorption from Pt(111) single-crystal surfaces after 2.0 L total doses at 110 K. The data correspond to enantiopure S-PO (a, bottom) and R-PO (a, top), to sequential doses of 0.5 L S-PO + 1.5 L R-PO (b, bottom) and 0.5 L R-PO + 1.5 L S-PO (b, top), and to racemic normal (c, bottom) and perdeutero (c, top) PO. The signal for 58 amu was followed in all cases except for Rac-PO-*d*₆, for which the signal for 64 amu was used instead. The areas of the molecular desorption peaks from the monolayer, the features at 193–195 K, were used to determine the saturation coverages. It was found that the TPD peak areas from the enantiopure samples are 15–20% larger than those from the enantiomeric mixtures.

the sticking probabilities of PO increase with coverage in the early stages of the uptake, reflecting an adsorption process aided by the presence of other adsorbates on the surface. It was also determined that these interactions are different with homo- versus hetero enantiomeric pairs. Kinetic Monte Carlo simulations that incorporate these effects qualitatively reproduced the experimental measurements and highlighted the kinetic driving force for the differences observed. This type of kinetic enantioselectivity in sticking coefficients could explain the preferential crystallization of one of the two enantiomers of a given chiral compound seen in some systems,^{8–10} and could potentially be exploited to design kinetically controlled chiral resolution schemes.

2. EXPERIMENTAL DETAILS

All experiments other than the STM were carried out in a small molecular-beam apparatus described in detail in previous publications.^{11,12} Briefly, the Pt(111) single crystal is mounted on a manipulator capable of *x*-*y*-*z*-*θ* motion, of cooling to liquid-nitrogen temperatures, and of resistive heating up to approximately 1250 K. The crystal is placed in an ultrahigh vacuum (UHV) chamber turbopumped to a base pressure of about 2×10^{-10} Torr. The temperature of the crystal is measured by using a chromel-alumel thermocouple spot-welded to the side of the crystal, and monitored and controlled by using homemade electronics. Linear heating ramps of 10 K/s are used for the TPD experiments, and constant fixed temperatures are set for the molecular beam uptakes. The front surface of the crystal is cleaned by a combination of ion sputtering and chemical treatments with O₂ before each experiment. A UTI quadrupole mass spectrometer, placed in the back of the chamber and interfaced to a personal computer, is used to follow the gas composition during the TPD and molecular beam experiments. The kinetic experiments were performed by using an effusive collimated molecular beam

generated by a 1.2-cm-diameter multichannel microcapillary array. A stainless-steel flag is used in this setup to block and unblock the beam at will. The STM images were acquired in a second UHV chamber by using an Omicron Nanotechnology variable-temperature scanning tunneling microscope (VT-UHV-STM).¹³ The base pressure in the STM chamber was less than 1×10^{-10} Torr. STM images were acquired with either Omicron or Veeco etched W tips. The scanning conditions used to acquire the PO/Pt(111) images were -1 to +1 V and 5 to 200 pA, where the scanning bias was applied to the sample.

The gases, argon (Liquid Carbonic 99.999% purity) and oxygen (Nellcor Puritan Bennett, 99.5% purity) for cleaning and propylene oxide-*d*₆ (Sigma Aldrich, 99% purity, 98 D atom % D) for the isotope-labeling experiments, were used as supplied. The liquid R-, S-, and Rac-propylene oxides (PO, Sigma Aldrich 99% purity) were subjected to several freeze-pump-thaw cycles for purification before use. Dosing was achieved by introducing controlled amounts of the vapors into the UHV chambers using leak valves. This was carried out at surface temperatures of approximately 30 K in the STM studies and 110 K in all other experiments unless otherwise indicated, and reported in langmuirs (1 L $\equiv 10^{-6}$ Torr × s). Doses were not corrected for differences in ion gauge sensitivities. The conversion of exposures to surface coverages was done by using the data from a series of TPD calibration experiments with each PO enantiomer as a function of dose. The absolute signals from the TPD and molecular beam signals (used to obtain absolute surface coverages for the PO) were also calibrated against data obtained for carbon monoxide adsorption, corrected for differences in ion gauge and mass spectrometry sensitivities. TPD and molecular beam data are reported here only for one enantiopure PO (generally S-PO), but similar experiments were carried out with the opposite enantiomer (or pair of enantiomers in the case of the sequential dosings) to check

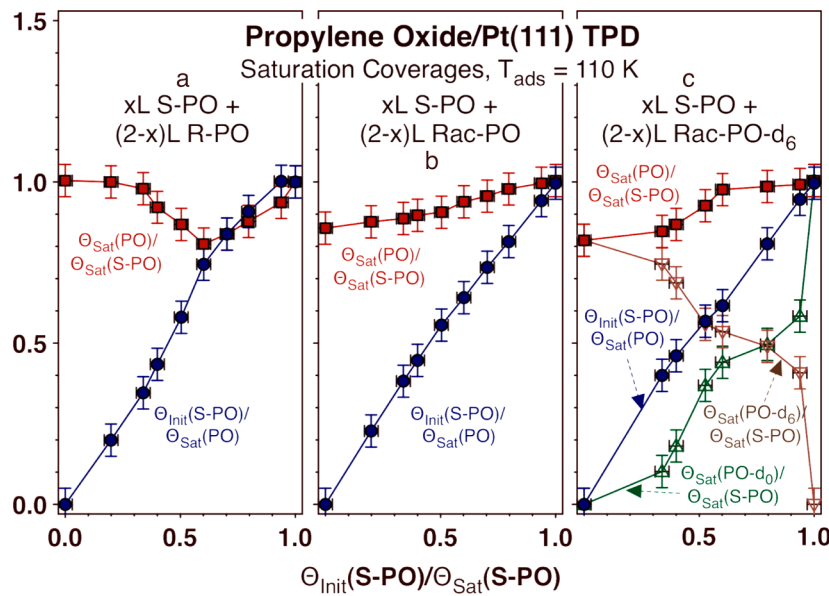


Figure 2. Summary of TPD area data from experiments such as those reported in Figure 1 for surfaces first dosed with varying amounts of S-PO and then with R-PO (a), Rac-PO (b), or Rac-PO- d_6 (c) until reaching a 2.0 L total exposure. The data are shown as a function of the initial surface coverage of S-PO, estimated from an independent calibration of coverage versus exposure. The red filled squares report the total PO saturation coverages measured in each case, whereas the blue filled circles correspond to the nominal initial S-PO coverages referenced to those saturation coverages. A minimum in saturation coverage is seen in all cases for racemic mixtures on the surface, at a value about 20% below the number for the enantiopure PO. The data in panel a appears to be skewed toward higher S-PO initial coverages, but that is because some of the initial adsorbates are displaced by the new incoming molecules, as highlighted in the experiments with the isotope-labeled Rac-PO- d_6 . (c) The final coverages for S-PO- d_6 (green open upward-pointing triangles) clearly deviate from the initial values shown by the blue filled circles and are compensated by the PO- d_6 adsorbates (brown open downward-pointing triangles).

that there were no experimental artifacts due to impurities or other factors. Experiments with the racemic mixtures were performed with both a commercial sample and S-PO + R-PO mixtures made in house.

The Monte Carlo simulations were carried out by using a home-written routine in Matlab. The adsorption of the PO molecules was simulated on a 200×200 square lattice with periodic boundaries, and run for 1×10^6 events to ensure that the surface reached saturation. The POs were represented as “L” shaped molecules surrounded by a one-lattice-space frame (shown as white squares in Figure 4c) to prevent adsorption of molecules directly touching each other. Different intrinsic sticking probabilities (S_o) were assigned to empty ($S_o(\text{Empty}) = 0.01$) versus occupied ($S_o(\text{Occupied}) = 0.99$) sites, as indicated in Figure 4b, and specific adsorption geometries were defined for incoming molecules hitting on adsorbates depending on their relative handedness (S-S or R-R versus S-R or R-S). More details are provided in the Supporting Information. The data in Figure 4 panels b and c correspond to a single run, but those were repeated several times to corroborate the trends observed: saturation coverages could be reproduced this way with an accuracy of better than 1%.

3. RESULTS

The first piece of evidence obtained in our studies for the differences in monolayer density between enantiopure and racemic PO layers on Pt(111) came from TPD data such as those shown in Figure 1. The general aspects of the adsorption of PO have already been characterized in detail on both Pt(111)¹⁴ and Pd(111)¹⁵ single-crystal surfaces. It has been determined that the adsorption at low temperatures is molecular and that molecular desorption occurs in two stages, at approximately 145 and 195 K from condensed multilayers

and the first monolayer on Pt(111), respectively. The data in Figure 1 are consistent with those observations. In addition, it also became clear from careful analysis of our TPD traces that the areas under the monolayer peaks, which are proportional to the PO saturation coverages on the Pt(111) surface, are different for enantiopure (Figure 1a) versus racemic (Figure 1c) PO layers: the latter are somewhere between 15 and 20% lower than the former. This is also true for surface monolayers prepared by sequential dosing of one enantiomer followed by the other (Figure 1b). It is worth noting that the TPD peak positions do not change with the enantiocomposition of the surface layer, they are all centered at about 193–195 K; only their intensities are seen to vary. This indicates that the adsorption energies (or, more precisely, the Gibbs free energies for the desorption kinetics) are the same for the enantiopure and mixed PO layers.

It was found that the decrease in saturation coverage in going from enantiopure to racemic PO monolayers is smooth, and occurs monotonically as the ratio of enantiomers on the surface varies from 1:0 to 0.5:0.5. This is illustrated by the data in Figure 2. In Figure 2a, the relative saturation coverage was tuned by varying the initial dose of the first enantiomer (S-PO), after which the surface was saturated with the other (R-PO). A clear minimum is seen in that figure for an initial S-PO coverage of ~60% of saturation, which in fact amounts to a nominal ~75% of the final mixed-layer saturation coverage because that is lower than the saturation coverage of the pure S-PO. The saturation coverage then returns slowly to its maximum value with increasing S-PO predose past the 60% point. A similar minimum saturation coverage is obtained by using a racemic PO mixture, and a monotonic increase is observed if decreasing submonolayer coverages of Rac-PO are supplemented by the addition of a pure enantiomer (S-PO) to

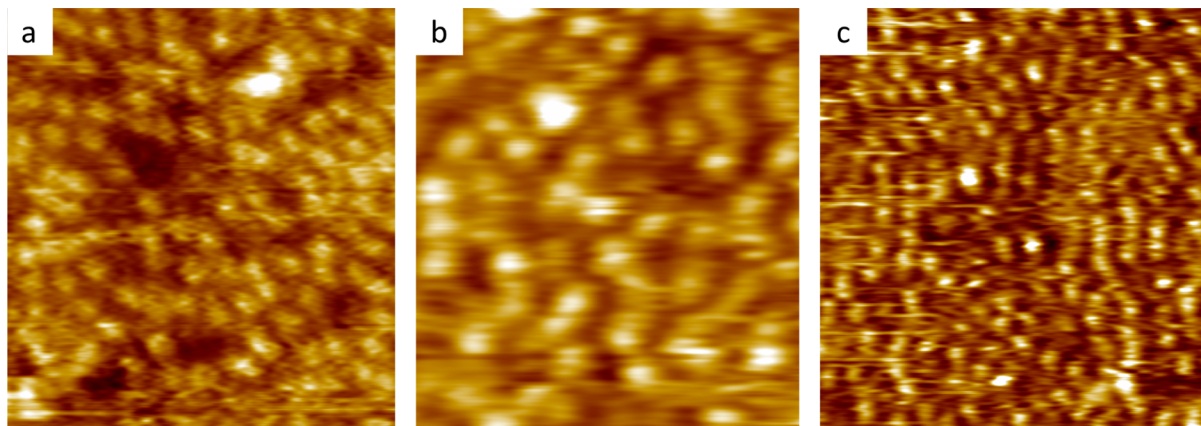


Figure 3. Scanning tunneling microscopy (STM) images for saturated layers of PO adsorbed on a Pt(111) single crystal. Images a and b correspond to 12.0 L of R-PO and Rac-PO, respectively, dosed at 30 K and then annealed at 120 K. Image (c) corresponds to a 60.0 L exposure of Rac-PO at 170 K. The Rac-PO layers are less dense than those obtained with R-PO, but can be made denser by carrying out the dosing at higher temperatures. No evidence for molecular pairing or for long-range ordering is observed in any case. All images correspond to areas of $6.4 \times 7.0 \text{ nm}^2$.

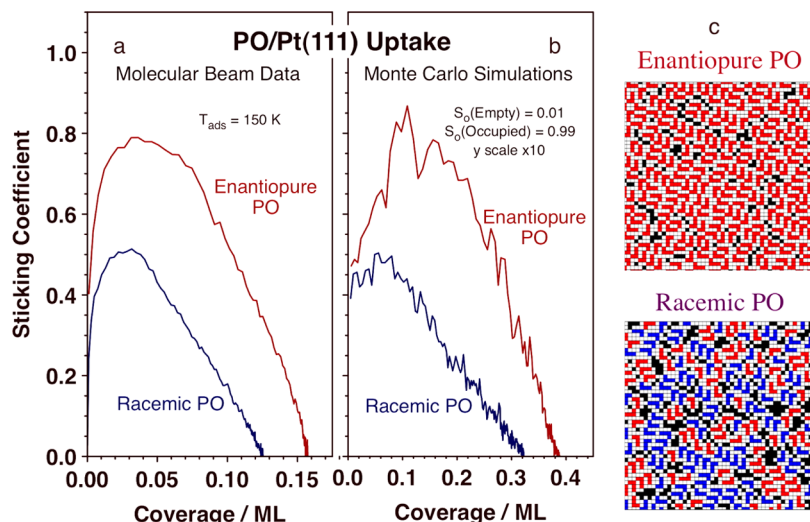


Figure 4. Experimental (a) and Monte Carlo-simulated (b) isothermal uptake curves for PO on Pt(111) in the form of sticking coefficient versus PO surface coverage. Two traces are shown in each panel, for the enantiopure (red) and racemic (blue) PO uptakes. Adsorption in the experimental molecular-beam data was carried out at 150 K. Higher saturation coverage and sticking coefficients are always seen with the enantiopure molecules compared to the racemic PO. There is also always an initial increase in sticking coefficient with coverage, reproduced in the Monte Carlo simulations by introducing an adsorbate-assisted process with a higher sticking coefficient on occupied sites, $S_o(\text{Occupied}) = 0.99$, than on empty sites, $S_o(\text{Empty}) = 0.01$. Panel c shows snapshots of the simulated surfaces obtained at saturation with enantiopure (top) and racemic (bottom) PO. The red and blue elements represent the two enantiomers of PO, the white squares the buffer zones used between adsorbates, and the black areas unfilled empty spaces.

reach saturation (Figure 2b). There seems to be an asymmetry in the data in Figure 2a, where the minimum saturation coverage is seen at an initial S-PO coverage measurably above one-half monolayer, but this can be easily explained by the partial displacement of adsorbates induced by the new incoming molecules, as highlighted by the isotope-labeling data in Figure 2c: only a fraction of the S-PO- d_0 dosed initially (blue filled circles) remains on the surface upon exposure to additional Rac-PO- d_6 (green open upper-pointing triangles), while about 20% is displaced by the new incoming molecules (brown open upper-pointing triangles).

The differences in saturation coverage with PO monolayer enantiocomposition measured by TPD are also evident in STM images such as those shown in Figure 3. For instance, Figure 3 panels a and b highlight the significant differences in adsorbate densities that are obtained by low-temperature dosing of

enantiopure versus racemic PO on the Pt(111) surface, respectively. It is also clear that, although the PO molecules may bond to specific sites in registry with the underlying platinum atoms within the Pt(111) surface, no ordered overlayers are formed; no long-range periodicity could be identified by 2D Fourier-transform analysis of the images. There is no obvious indication of any pairing pointing to strong intermolecular interactions in the enantiopure or the racemic surface layers either. The disorder seen in these surface layers leads to some fluctuations in local PO coverage on the surface (Figure S1, Supporting Information), but the differences in saturation coverage between the enantiopure and racemic cases are well beyond those margins of error. The saturation coverages for enantiopure and racemic PO were measured to be 2.4 ± 0.4 and 1.7 ± 0.7 molecules/ nm^2 , respectively, or 0.16 and 0.11 ML (1 ML = 1 molecule/Pt atom), values consistent

with those obtained by TPD and molecular beam experiments (Figure S2, Supporting Information).

Higher saturation coverage can be obtained with racemic PO if the dosing is carried out at higher temperatures and/or for longer times. Figure 3c shows an example of the type of higher-density layer that results from dosing at 170 K. This conclusion, which points to a kinetically rather than thermodynamically driven process, is supported by TPD data as well (Figure S3, Supporting Information). The results from TPD isotope-labeling experiments strongly suggest that the additional uptake is aided mainly by a continuous replacement of adsorbates via desorption–adsorption events, not by diffusion of the original adsorbates. This is surprising, because diffusion of adsorbed species typically displays activation barriers only 5 to 20% as high as those for desorption.¹⁶ In our case, the thermal packing of the layers is limited by the fact that at 170 K, the highest dosing temperature tested, significant molecular desorption is already observed from the monolayer (see TPD data in Figure 1).

To better understand the kinetics of the enantioselective PO adsorption phenomenon, isothermal measurements of the PO uptake were carried out with an effusive collimated molecular beam¹⁷ by using the King and Wells method.¹⁸ Typical raw data obtained at different temperatures are shown in Figure S4 (Supporting Information), and a detailed description of the data analysis procedure is provided in a previous reference.¹¹ Figure 4a displays the sticking coefficient (adsorption probability) curves versus coverage obtained by using this approach for both enantiopure and racemic PO on Pt(111) at 150 K. Not only is it clear from these data that the final saturation coverage is higher with enantiopure PO than with racemic PO, but it is also evident that the sticking coefficient is always higher with the enantiopure PO. This observation is repeated at all adsorption temperatures (Figure S5, Supporting Information). Perhaps more significantly, the sticking coefficients increase with coverage in the initial stages of the uptake in both cases, with both enantiopure and racemic PO. This is an unusual behavior, since the probability for adsorption typically decreases as surface sites are blocked by the adsorbates. It has nevertheless been observed in a few selected systems, and explained by adsorption dynamics assisted by adsorbates already present on the surface, perhaps via an adsorption precursor state that helps dissipate the excess kinetic energy of the incoming gas molecules.^{19,20} In our case, the sticking coefficients also proved to be dependent on the relative handedness of the PO molecules involved in each adsorption event. This is evidenced by the data in Figure 5, which shows the uptake curves for either R-PO (Figure 5a) or Rac-PO (Figure 5b) on surfaces precovered with varying amounts of S-PO. Again, the sticking coefficients of racemic PO are always lower than those of enantiopure PO, as discussed before. Additionally, the sticking coefficients evolve in different ways as a function of coverage: whereas the R-PO coverage at which the sticking coefficient reaches its maximum value is roughly independent of the S-PO precoverage, with Rac-PO it is mainly the total coverage (Rac-PO + S-PO) that determines that value. Also, the early behavior of the sticking coefficient versus Rac-PO coverage is similar regardless of the initial S-PO precoverage (the traces all overlap), whereas the absolute value of the sticking coefficient for R-PO decreases with increasing S-PO predose. Clearly, the sticking coefficient depends on the relative handedness of the incoming PO

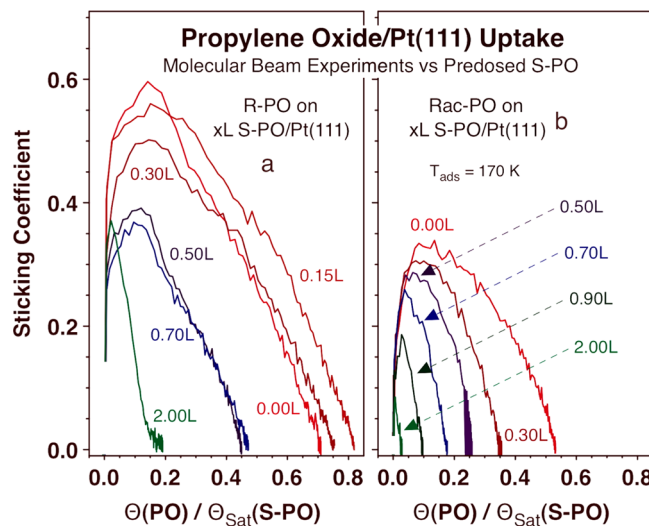


Figure 5. Isothermal uptake curves for PO on Pt(111) surfaces predosed with varying amounts of S-PO, as indicated in the labels for each curve. Data are reported for R-PO (a) and Rac-PO (b) adsorption at 170 K. Very different behavior and trends are seen in both cases, indicating a different interaction between the incoming and adsorbed PO molecules depending on their relative handedness (S–S or R–R versus S–R or R–S).

molecule relative to that of the adsorbed PO that assists in its uptake on the surface.

Kinetic Monte Carlo simulations including the factors identified above, namely, higher sticking coefficients on adsorbate-covered versus empty Pt(111) sites (to reflect the adsorbate-assisted behavior) and a different sticking geometrical behavior for homochiral S-PO(g) + S-PO(ads) or R-PO(g) + R-PO(ads) versus heterochiral S-PO(g) + R-PO(ads) or R-PO(g) + S-PO(ads) pairs, qualitatively reproduce the main features of the experimental uptake curves, namely, the higher saturation coverages and sticking coefficients seen for enantiopure versus racemic PO and the initial increase in sticking coefficient with coverage in the early stages of the adsorption. Examples of the simulated uptake kinetics for both racemic and enantiopure PO displaying these properties are shown in Figure 4b.

The calculations also point to a short-range correlation in the distribution of the adsorbates on the surface due to the adsorbate-assisted enhanced sticking, which leads to the formation of short linear chains. This chain formation is visually evident in the STM image in Figure 6a, and was corroborated by analysis of the statistical distribution of nearest neighbors obtained at submonolayer coverages of PO on the Pt(111) surface. Figure 6b shows how the observed arrangement of adsorbates deviates from that estimated by assuming a random distribution, with a clear excess of pairs of nearest neighbors seen in the experiments. The short chains can also be seen in the snapshots shown in Figure 4c, which displays the end-point surfaces obtained from the Monte Carlo simulations.

4. DISCUSSION

As reported above, the adsorption of PO on Pt(111) single-crystal surfaces behaves in an unexpected manner that is dependent upon its enantiomeric composition. First, the adsorbed PO appears to form chiral solutions all throughout the range of chiral ratios, from pure enantiomers to racemic mixtures: the PO saturation coverage varies smoothly with

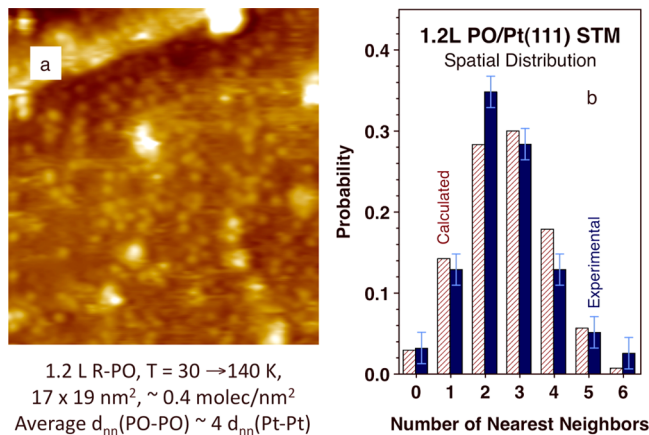


Figure 6. (a) STM image for a submonolayer coverage of R-PO on Pt(111), obtained by dosing 1.2 L of the PO at 30 K and annealing at 140 K. The image corresponds to a 17 × 19 nm² area, and shows an average molecular density of 0.4 molecules/nm² (or 0.03 ML) and an average nearest-neighbor PO-PO distance equivalent to approximately four Pt-Pt lattice distances. (b) Distribution of PO nearest-neighbors, calculated from the STM image and contrasted against the expected distribution from random adsorption. An excess of two nearest-neighbor adsorbates is seen in the experimental distribution, in qualitative agreement with the adsorbate-assisted sticking process included in the Monte Carlo simulations in Figure 4.

enantiomeric composition, and the same behavior is seen regardless of the adsorption procedure used, either by using premade mixtures or via the sequential dose of the two enantiomers. As mentioned in the introduction, such solutions are rare in three dimensions, amounting to less than 1% of the chiral systems characterized to date.^{2,4,5,7} Much less is known about two-dimensional adsorbed phases such as the one reported here, but the limited studies available to date point to analogous possibilities for the evolution of chiral adsorbates into racemates or conglomerates (perhaps with a higher probability toward conglomerates than in 3D).^{21–23} There have been some reports of racemic solutions on surfaces, but even in those cases the molecules display long-range order; only the local geometry of each individual adsorbate may show a random distribution of chiralities.^{24,25} In fact, this is another aspect of the behavior of our system worth highlighting: that the adsorbed species are disordered on the surface. Most chiral systems characterized to date form crystalline phases.²

In addition to the fact that the saturation layers of PO adsorbed on Pt(111) vary in density with chiral composition, it is worth noticing that the racemic layers are the ones that display significantly lower densities compared to those made out of enantiopure PO. This trend is opposite to that established long ago by Wallach, who claimed that the density of racemic mixtures should be higher than that of the pure enantiomers.^{26,27} His conclusion has in fact been challenged in several instances already; our example adds to that list of exceptions.^{27,28} What appears to be true regardless is that there is a correlation between the density of the solids and their melting properties: higher densities in racemates (versus conglomerates) correlate with higher melting points, and vice versa.²⁹ Once again, the PO/Pt(111) system deviates from that expected behavior: whereas the racemic PO layer displays lower surface saturation densities than the enantiopure PO counterpart, they both exhibit the same desorption energetics (as

indicated by the same desorption temperatures observed in the TPD experiments).

This latter apparent contradiction points to what may perhaps be the most important and unique aspect of the PO/Pt(111) system: the higher density observed for the saturated layer of enantiopure PO compared to that observed for the saturated layer of racemic PO is due to a kinetic, not thermodynamic, effect. The connection between crystal densities and melting points seen in other chiral cases has been explained in terms of strong intermolecular interactions such as hydrogen bonding, which can facilitate the formation of racemates,²⁹ and no evidence for molecular pairing or for strong intermolecular interactions was obtained in our studies. There are no indications from our data that there are any strong attractive or repulsive forces between adjacent PO adsorbates, either in the enantiopure or in the racemic PO layers. At the other end of the spectrum, ideal chiral solutions should have the same melting point as enantiopure samples because the enthalpy of mixing is zero,² like in our case, but those systems are not expected to display any density variations, and here the densities of the racemic and enantiopure layers are different. These contradictions cannot be easily explained by thermodynamics.

Several pieces of evidence can be recalled to justify the conclusion that the reported differences in PO saturation coverage on Pt(111) surfaces are the result of unique adsorption kinetics. First, it was observed that the saturation coverage of racemic PO layers could be increased by increasing the temperature of adsorption and/or the exposure time. Interestingly, the extra surface packing that results from such an approach appears to be the result of multiple desorption-adsorption events rather than a consequence of surface diffusion. For reasons not fully understood at present, the diffusion of surface adsorbates in this case is severely hindered, and is minimal even at the temperatures required for molecular desorption. Second, it was determined that the kinetics of the uptake are affected by the adsorbates on the surface. This adsorbate-assisted sticking of molecules from the gas phase has been reported before but it is not common,^{19,20} and in our case is further complicated by the fact that there is an added difference between the kinetics of adsorption of PO molecules on or nearby sites occupied by another PO molecule of the same versus the opposite chirality. This is the property that, according to our Monte Carlo simulations, accounts for the differences in monolayer density with varying PO enantiomeric excess. To the best of our knowledge, this behavior is unprecedented in the literature.

The observations and conclusions reported here may well prove broadly applicable to other systems. In fact, it may be that kinetic effects such as those reported here explain the cross-crystallization that has been reported for some chiral systems.⁸ In particular, it has been shown that the crystallization of one enantiomer on another may be kinetically favored either by seeding⁹ or by using surface-modifying additives.¹⁰ According to the theory of interface-controlled crystal growth, the overall growth rate depends on both the rate at which molecules arrive at the growth interface (R_1) and the rate at which molecules at the growth interface enter the crystal lattice (R_2).³⁰ For two enantiomers in the same melt, R_1 must be the same, which means that R_2 should be different, and that is the rate for which our adsorbate-assisted sticking may be relevant. In this context, the higher sticking coefficients reported here for the adsorption of enantiomers on layers of adsorbates with the

same (versus the opposite) enantiomer could potentially be used to design preferential condensation schemes for chiral resolutions.^{2,31–34} It does remain to be determined how general the type of enantiospecific adsorbate-assisted adsorption kinetics reported here may be.

■ ASSOCIATED CONTENT

S Supporting Information

STM images showing spatial fluctuations in PO surface coverage, estimated PO absolute coverage data, PO displacement kinetics versus temperature and time, raw molecular-beam S-PO uptake data versus time for four temperatures, sticking coefficient versus coverage, R_s and Rac-PO for four temperatures, and details on the Monte Carlo simulations. This material is available free of charge via the Internet at <http://pubs.acs.org>.

■ AUTHOR INFORMATION

Corresponding Author

*E-mail: zaera@ucr.edu.

Notes

The authors declare no competing financial interest.

■ ACKNOWLEDGMENTS

Financial support for this project was provided by the U.S. Department of Energy, Office of Basic Energy Sciences, grant DE-FG02-12ER16330. T.J.L., F.R.L., and E.C.H.S. thank the National Science Foundation for support (CHE-1012307). S.K. and F.Z. would also like to thank Prof. Gregory Beran for his help in setting up the Monte Carlo simulations.

■ REFERENCES

- (1) Blaser, H. U.; Spindler, F.; Studer, M. Enantioselective Catalysis in Fine Chemicals Production. *Appl. Catal., A* **2001**, *221*, 119–143.
- (2) Jacques, J.; Collet, A.; Wilen, S. H. *Enantiomers, Racemates and Resolutions*; Krieger: New York, 1994.
- (3) Corvis, Y.; Negrier, P.; Massip, S.; Leger, J.-M.; Espeau, P. Insights into the Crystal Structure, Polymorphism, and Thermal Behaviour of Menthol Optical Isomers and Racemates. *CrystEngComm* **2012**, *14*, 7055–7064.
- (4) Collet, A. Separation and Purification of Enantiomers by Crystallisation Methods. *Enantiomer* **1999**, *4*, 157–172.
- (5) Srisanga, S.; ter Horst, J. H. Racemic Compound, Conglomerate, or Solid Solution: Phase Diagram Screening of Chiral Compounds. *Cryst. Growth Des.* **2010**, *10*, 1808–1812.
- (6) Pasteur, L. Recherches sur les Relations qui Peuvent Exister entre la Forme Cristalline, la Composition Chimique, et la Sens de la Polarisation Rotatoire. *Ann. Chem.* **1848**, 442–459.
- (7) Taratin, N. V.; Lorenz, H.; Kotelnikova, E. N.; Glikin, A. E.; Galland, A.; Dupray, V.; Coquerel, G.; Seidel-Morgenstern, A. Mixed Crystals in Chiral Organic Systems: A Case Study on (R)- and (S)-Ethanolammonium 3-Chloromandelate. *Cryst. Growth Des.* **2012**, *12*, 5882–5888.
- (8) Yu, L. Nucleation of One Polymorph by Another. *J. Am. Chem. Soc.* **2003**, *125*, 6380–6381.
- (9) Huang, J.; Chen, S.; Guzei, I. A.; Yu, L. Discovery of a Solid Solution of Enantiomers in a Racemate-Forming System by Seeding. *J. Am. Chem. Soc.* **2006**, *128*, 11985–11992.
- (10) Weissbuch, I.; Lahav, M.; Leiserowitz, L. Toward Stereochemical Control, Monitoring, and Understanding of Crystal Nucleation. *Cryst. Growth Des.* **2003**, *3*, 125–150.
- (11) Liu, J.; Xu, M.; Nordmeyer, T.; Zaera, F. Sticking Probabilities for CO Adsorption on Pt(111) Surfaces Revisited. *J. Phys. Chem.* **1995**, *99*, 6167–6175.
- (12) Wilson, J. N.; Zaera, F. Alkane Oxidation on Rh(111) Single-Crystal Surfaces under High-Temperature, Short-Contact-Time Conditions: A Molecular Beam Kinetic Study. *J. Phys. Chem. C* **2010**, *114*, 16946–16954.
- (13) Mhatre, B. S.; Pushkarev, V.; Holsclaw, B.; Lawton, T. J.; Sykes, E. C. H.; Gellman, A. J. A Window on Surface Explosions: Tartaric Acid on Cu(110). *J. Phys. Chem. C* **2013**, *117*, 7577–7588.
- (14) Lee, I.; Zaera, F. Enantioselectivity of Adsorption Sites Created by Chiral 2-Butanol Adsorbed on Pt(111) Single-Crystal Surfaces. *J. Phys. Chem. B* **2005**, *109*, 12920–12926.
- (15) Stacchiola, D.; Burkholder, L.; Tysoe, W. T. Enantioselective Chemisorption on a Chirally Modified Surface in Ultrahigh Vacuum: Adsorption of Propylene Oxide on 2-Butoxide-Covered Palladium(111). *J. Am. Chem. Soc.* **2002**, *124*, 8984–8989.
- (16) Zangwill, A. *Physics at Surfaces*; Cambridge University Press: Cambridge, 1988.
- (17) Zaera, F. Infrared and Molecular Beam Studies of Chemical Reactions on Solid Surfaces. *Int. Rev. Phys. Chem.* **2002**, *21*, 433–471.
- (18) King, D. A.; Wells, M. G. Molecular Beam Investigation of Adsorption Kinetics on Bulk Metal Targets: Nitrogen on Tungsten. *Surf. Sci.* **1972**, *29*, 454–482.
- (19) Bowker, M.; King, D. A. Anomalous Adsorption Kinetics. g-Nitrogen on the {110} Plane of Tungsten. *J. Chem. Soc., Faraday Trans. 1* **1979**, *75*, 2100–2115.
- (20) Arumainayagam, C. R.; McMaster, M. C.; Madix, R. J. Coverage Dependence of Molecular Adsorption Dynamics: Ethane on Platinum (111). *J. Phys. Chem.* **1991**, *95*, 2461–2465.
- (21) Perez-Garcia, L.; Amabilino, D. B. Spontaneous Resolution, Whence and Whither: From Enantiomorphic Solids to Chiral Liquid Crystals, Monolayers and Macro- and Supra-Molecular Polymers and Assemblies. *Chem. Soc. Rev.* **2007**, *36*, 941–967.
- (22) Mark, A. G.; Forster, M.; Raval, R. Direct Visualization of Chirality in Two Dimensions. *Tetrahedron: Asymmetry* **2010**, *21*, 1125–1134.
- (23) Ernst, K.-H. Molecular Chirality at Surfaces. *Phys. Status Solidi B* **2012**, *249*, 2057–2088.
- (24) Romer, S.; Behzadi, B.; Fasel, R.; Ernst, K.-H. Homochiral Conglomerates and Racemic Crystals in Two Dimensions: Tartaric Acid on Cu(110). *Chem.—Eur. J.* **2005**, *11*, 4149–4154.
- (25) Mark, A. G.; Forster, M.; Raval, R. Recognition and Ordering at Surfaces: The Importance of Handedness and Footedness. *Chem.-PhysChem* **2011**, *12*, 1474–1480.
- (26) Wallach, O. Zur Kenntnis der Terpene und der Ätherischen Ole. *Justus Liebigs Ann. Chem.* **1895**, *286*, 90–118.
- (27) Brock, C. P.; Schweizer, W. B.; Dunitz, J. D. On the Validity of Wallach's Rule: On the Density and Stability of Racemic Crystals Compared with Their Chiral Counterparts. *J. Am. Chem. Soc.* **1991**, *113*, 9811–9820.
- (28) Cai, W.; Marciniak, J.; Andrzejewski, M.; Katrusiak, A. Pressure Effect on D,L-Mandelic Acid Racemate Crystallization. *J. Phys. Chem. C* **2013**, *117*, 7279–7285.
- (29) Sørensen, H. O.; Larsen, S. Hydrogen Bonding in Enantiomeric versus Racemic Mono-Carboxylic Acids: A Case Study of 2-Phenoxy-Propionic Acid. *Acta Crystallogr. B* **2003**, *59*, 132–140.
- (30) *Changes of State*; Hannay, N. B., Ed.; Springer: New York, 1975; Vol. 5.
- (31) Lorenz, H.; Polenske, D.; Seidel-Morgenstern, A. Application of Preferential Crystallization To Resolve Racemic Compounds in a Hybrid Process. *Chirality* **2006**, *18*, 828–840.
- (32) *Novel Optical Resolution Technologies*; Sakai, K.; Hirayama, N.; Tamura, R., Eds.; Springer-Verlag: Berlin, 2007; Vol. 269.
- (33) Coquerel, G. Preferential Crystallization. *Top. Curr. Chem.* **2007**, *269*, 1–51.
- (34) Haq, S.; Liu, N.; Humblot, V.; Jansen, A. P. J.; Raval, R. Drastic Symmetry Breaking in Supramolecular Organization of Enantiomerically Unbalanced Monolayers at Surfaces. *Nat. Chem.* **2009**, *1*, 409–414.